Molecular Physics, 2015
Vol. 113, Nos. 13–14, 1768–1779, http://dx.doi.org/10.1080/00268976.2015.1012131

INVITED ARTICLE

Computation of molecular parity violation using the coupled-cluster linear response approach

Ľuboš Horný and Martin Quack*

Laboratory of Physical Chemistry, ETH Zürich, CH-8093 Zürich, Switzerland

(*Received 22 December 2014; accepted 20 January 2015*)

In memoriam, Nicholas C. Handy.

We report the implementation of a coupled-cluster linear response approach for the computation of molecular parity violation (in the framework of the PSI3 code, in particular). The approach is applied first to molecules such as hydrogen peroxide (HOOH), hydrogen disulfide (HSSH) and dichlorinedioxide (ClOOCl), which have been studied previously. The importance of including correlation is demonstrated for these examples, also including selected variations of geometry providing parity violation as a function of torsional angles. For the substituted allenes, 1,3 difluoroallene (CHF=C=CHF), 1,fluoro,3 chloroallene (CHF=C=CHCl) and 1,3 dichloroallene (CHCl=C=CHCl), we find that in particular the last molecule may be a suitable candidate for the experimental study of molecular parity violation.

Keywords: molecular parity violation; parity violating potentials; coupled-cluster theory; enantiomers; axially chiral molecules; HOOH; HSSH; ClOOCl; allenes; CHF=C=CHF; CHCl=C=CHF; CHCl=C=CHCl; spectroscopy

1. Introduction

Space inversion symmetry (or 'parity symmetry P') is among the important discrete symmetries in physics and its violation accordingly among the most fundamental phenomena [1]. Measurements of parity-violating effects in heavy atoms have been used, following early proposals in the 1970's [2,3], as a test of the electroweak part of the standard model of particle physics (SMPP) [4–8] in the low-energy regime [9]. Parity violation or 'non-conservation' in atoms and molecules originates from the weak neutral currents associated with the exchange of the Z^0 boson between the atomic electron and nucleus. Soon after the discovery of parity violation in nuclear physics [10–13], speculations appeared concerning the possible consequences arising for molecular physics and chemistry including biomolecular homochirality [14–16]. Violation of parity symmetry by the weak neutral current removes the energetic degeneracy between the enantiomers, and correspondingly, induces a small energy difference between R and S enantiomers of a chiral molecule. For some prototypical and experimentally accessible chiral molecules this difference is currently estimated to be approximately 100 aeV(corresponding to a reaction enthalpy for stereomutation, $\Delta_{\mathrm{pv}} H_0^{\ominus} = 10^{-11}$ J mol^{-1} in CHFClBr, for example [1,17,18]). There have been several proposals to measure parity-violating effects in molecules. However, none of the experimental attempts to confirm the parity-violating effects in molecules have met so far with success [1,17,19–34]. The extent of molecular parity violation was initially estimated via theory, and accurate theoretical predictions of molecular parity violation are crucial in a search of molecular systems most suitable for the experiment. Early quantitative work appeared after about 1980 [35–37], but the early results were later found to be too small by about two orders of magnitude for the prototype molecules HOOH and HSSH [38]. These theoretical results [38–40], later confirmed [41–44], provided new impetus and hope for successful experiments. Over the last decade, further progress has been made [1,45–48] in the precise theoretical description of molecular-parity violation, its role in the stereomutation dynamics of chiral molecules and possible implications for the origin of molecular chirality and biomolecular homochirality. Experimentally, there are currently two different routes pursued [1]. In the first one, originally proposed by Letokhov [19], one attempts to carry out a high-resolution spectroscopic measurement of enantiomerically pure substances and observe frequency differences, $(\nu_{\mathrm{M}} - \nu_{\mathrm{P}})$ in Figure 1, between the corresponding spectral lines of two enantiomers. This would provide a difference of the parity-violating energy differences $(\Delta_{\mathrm{pv}}E - \Delta_{\mathrm{pv}}E^{*})$. In the second approach, proposed in [24,25], one uses an intermediate excited state of well-defined parity (the highest line marked + for positive parity in Figure 1), which can be connected by optical transition to the ground state of R and S (or P and M) enantiomers. One can then either observe a combination difference or the time-resolved transformation of an initial state with well-defined parity to a state of opposite parity in a pump-probe setup [1,49]. This second approach allows one

---

*Corresponding author. Email: martin@quack.ch

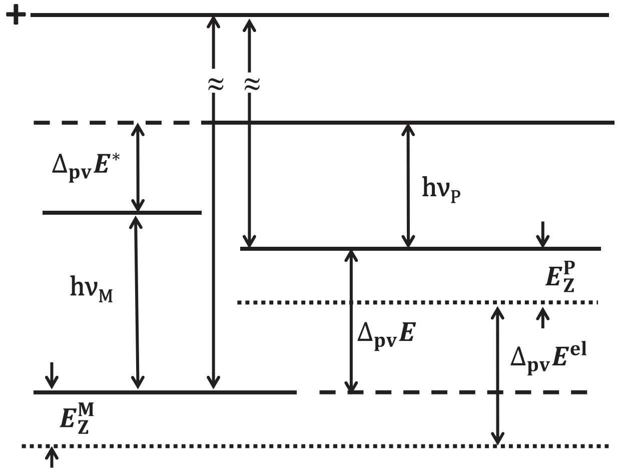

Figure 1. Energy-level diagram for 'left' M and 'right' P enantiomers of a chiral molecule. The dotted lines indicate the electronic potential-energy minima including parity-violating potentials, whereas the solid lines indicate vibrational (ground and excited) state levels including zero-point energy (E_Z) and parity-violating corrections (not to scale). The transitions (vertical lines) to the broken lines are forbidden, whereas transitions between solid lines are observable spectroscopically(modified after [45]).

to determine the parity-violating energy difference $\Delta_{\mathrm{pv}}E$ between enantiomers. Figure 1 illustrates the energy-level scheme relevant to the two approaches. There have been further proposals [16,22,23,26], but none of these seem to be currently pursued. The two approaches that are actively pursued in a few laboratories, as described above, require that the parity-violating energy difference $\Delta_{\mathrm{pv}}E$ is much larger than the tunneling splitting $\Delta E_{\pm}$ in the hypothetical symmetric case [1]. This condition is frequently fulfilled, certainly so for all chiral molecules that exist as a stable enantiomers for a time of days and more [1]. In practice, preparing for such experiments, one needs to have good prior theoretical estimates of the expected effects for a particular molecule. Since the planned experiments are expected to be very difficult, a guidance to the most fitting molecular prototypes and the ability to select a particularly suitable molecule are desirable. In this context, we and others have continued theoretical developments for reliably calculating parity-violating potentials in polyatomic molecules. This paper aims at providing a further progress along these lines towards a more accurate computation of parity violation and a coupled-cluster approach appeared promising.

Today, some of the most accurate results among the electronic structure theories are achieved with the coupled-cluster theory, which was originally presented [50] by Čížek, being inspired by earlier work on the theory of nuclear matter [51] and electron pairs correlation [52], and initially applied [50,53,54] by Čížek and Paldus. Numerous further developments (for details see several reviews [55–59] and books [60–63]) have made this approach one of the most frequently applied methods for precise quantum chemical calculations of structure, energies and properties [64–78] of molecules at configurations which do not depart too much from the equilibrium geometry towards the dissociation, but allowing for large amplitude motions with conformational changes [79,80]. This method is thus ideally suited to calculate accurate expectation values for parity-violating potentials of polyatomic (chiral) molecules and clusters for the ground state and lower excited vibration–rotation–tunnelling states, needed for planning experiment [1,49]. We thus decided to implement the coupled-cluster theory for parity violation in the open source program PSI3 [81].

We report here, the computation of molecular parity-violation potentials E_{pv} obtained as a static linear response function of parity-violating and spin–orbit (SO) coupling operators. We examine the importance of electron correlation for the parity-violating potentials. We present results for HOOH and HSSH, often studied prototype molecules in this context, and compare them with previous results obtained without inclusion of electron correlation or based on relativistic wavefunctions. Furthermore, we report new results for more complex systems, ClOOCl and the fluoro, chloro-substituted allenes(CHF=C=CHF, CHF=C=CHCl, CHCl=C=CHCl). We might note here that HOOH does not satisfy the condition $\Delta_{\mathrm{pv}}E \gg \Delta E_{\pm}$ (one rather has $\Delta_{\mathrm{pv}}E \ll \Delta E_{\pm} \cong hc$ 10 cm^{-1}). However, HOOH has been frequently used as prototype for both calculating the tunnelling [82–86] and parity violation. A preliminary account of our work was reported in [87].

2. Methods

The parity-violating electron–nucleus interaction operator $\hat{H}_{\mathrm{pv}}$ of a molecular system with N nuclei and n electrons can be within the non-relativistic framework expressed [1–3,35,39–41,88] (here in SI units):

$$\begin{aligned}
\hat{H}_{\mathrm{pv}}^{(\mathrm{e-nucl})} &= \hat{H}_{\mathrm{pv},1}^{(\mathrm{e-nucl})} + \hat{H}_{\mathrm{pv},2}^{(\mathrm{e-nucl})} + \hat{H}_{\mathrm{pv},3}^{(\mathrm{e-nucl})} \\
&= \sum_{i=1}^{n} \left(\hat{h}_{\mathrm{pv},1}^{(i)} + \hat{h}_{\mathrm{pv},2}^{(i)} + \hat{h}_{\mathrm{pv},3}^{(i)} \right) \\
&= \frac{\pi G_{\mathrm{F}}}{m_{\mathrm{e}} h c \sqrt{2}} \sum_{i=1}^{n} \Bigg[\sum_{A=1}^{N} Q_{\mathrm{w}}(A) \left\{ \hat{\vec{p}}_i \cdot \hat{\vec{s}}_i , \delta^3 (\vec{r}_i - \vec{r}_A) \right\} \\
&\quad + \sum_{A=1}^{N} (-\lambda_A) \left(1 - 4 \sin^2 \theta_{\mathrm{w}}\right) \left\{ \hat{\vec{p}}_i \cdot \hat{\vec{I}}_A , \delta^3 (\vec{r}_i - \vec{r}_A) \right\} \\
&\quad + \sum_{A=1}^{N} 2\mathrm{i}\lambda_A \left(1 - 4 \sin^2 \theta_{\mathrm{w}}\right) \left(\hat{\vec{s}}_i \times \hat{\vec{I}}_A \right) \\
&\quad \cdot \left[\hat{\vec{p}}_i , \delta^3 (\vec{r}_i - \vec{r}_A) \right]_{-} \Bigg],
\end{aligned} \tag{1}$$

where $G_F = 1.438586 \times 10^{-62}\, Jm^3$ is the 'Fermi' constant [89], m_{e} is the mass of electron, h is the Planck constant, c

is the speed of light, $\mathrm{i} = \sqrt{-1}$, $\hat{\hat{p}}_i$ and $\hat{\hat{s}}_i$ are the momentum and spin operators of electron i, $\hat{\hat{I}}_A$ is the reduced nuclear spin operator of nucleus A, $\delta^3(\vec{r}_i - \vec{r}_A)$ is the Dirac delta distribution, $\vec{r}_i$ and $\vec{r}_A$ are position vectors of electrons and nuclei, coefficient $\lambda_A \approx 1$ is a nuclear state-dependent factor close to unity. The electroweak charge $Q_\mathrm{w}(A)$ of nucleus A containing Z_A protons and N_A neutrons is

$$Q_\mathrm{w}(A) \approx (1 - 4\sin^2\theta_\mathrm{w})Z_A - N_A, \tag{2}$$

with θ_w the Weinberg angle and $\sin^2\theta_\mathrm{w} \approx 0.2319$. In Equation (1), the small contributions arising from the electron–electron weak interaction [39] are neglected. The first, nuclear spin-independent term $\hat{H}_{\mathrm{pv},1}^{(\mathrm{e-nucl})}$ is dominant for the calculation of parity-violating potentials of chiral molecules because of the usually large value of $Q_\mathrm{w}(A)$ for the relevant atoms in the molecules under consideration and because of the small prefactor $1 - 4\sin^2\theta_\mathrm{w} = 0.0724$ of the nuclear spin-dependent terms $\hat{H}_{\mathrm{pv},2}^{(i)}$ and $\hat{H}_{\mathrm{pv},3}^{(i)}$, which are not further considered here. These are, however, important for the calculation of parity-violating effects in nuclear magnetic resonance (NMR) spectra of chiral molecules [88,90–94]. Since $\hat{H}_{\mathrm{pv}}^{(\mathrm{e-nucl})}$ is a purely imaginary operator, its expectation values for the closed shell singlet states are zero. Considering the SO coupling, which is expected to account for the largest first-order correction to the molecular wavefunction, a non-vanishing parity-violating potential can be expressed [35,39,41,95] via perturbation theory as

$$E_\mathrm{pv} = 2\mathrm{Re}\left\{\sum_{n\neq 0}^{\infty} \frac{\langle\Psi_0|\hat{H}_\mathrm{pv}|\Psi_n\rangle\langle\Psi_n|\hat{H}_\mathrm{SO}|\Psi_0\rangle}{E_0 - E_n}\right\}, \tag{3}$$

where $|\Psi_0\rangle$ is the reference state of interest (usually the singlet ground state) with the corresponding energy E_0, and $|\Psi_n\rangle$ is the nth excited triplet state with energy E_n. The SO interaction operator in the Breit–Pauli form [41,96–99] can be written as

$$\hat{H}_\mathrm{SO} = \frac{e^2\hbar^2\mu_0}{8\pi m_\mathrm{e}^2}\left[\sum_{i=1}^{n}\sum_{A=1}^{N} Z_A \frac{\hat{\hat{l}}_{i,A}\cdot\hat{\hat{s}}_i}{|\vec{r}_A - \vec{r}_i|^3} - \sum_{i=1}^{n}\sum_{i\neq j}^{n} \frac{\hat{\hat{l}}_{i,j}\left(\hat{\hat{s}}_i + 2\hat{\hat{s}}_j\right)}{|\vec{r}_i - \vec{r}_j|^3}\right], \tag{4}$$

where $\hat{\hat{l}}_{i,A} = (\vec{r}_i - \vec{r}_A)\hat{\hat{p}}_i$ is the orbital angular momentum operator of the electron i. In the following, we do consider only the one-electron part of the SO coupling operator with effective nuclear charges Z_eff [100,101] as proposed earlier [39,40], an extension including the two-electron part being possible [41,102]. Having an SO coupling as the static perturbation, the parity-violating potential E_pv can be treated as a second-order property, and computed as a linear response function. We employ the coupled perturbed Hartree–Fock (CPHF) method [79,80] for the Hartree–Fock wavefunction, and the coupled-cluster linear response (CC-LR) method for the correlated, coupled-cluster wavefunctions. The CPHF method is equivalent to a static (zero frequency) limit of random phase approximation. The parity-violating potential E_pv is

$$E_\mathrm{pv} = \langle\langle \hat{H}_\mathrm{pv}; \hat{H}_\mathrm{so}\rangle\rangle_{\omega=0} = \overrightarrow{H_\mathrm{pv}}\ \mathbf{\Gamma}^{-1}\ \overrightarrow{H_\mathrm{so}}, \tag{5}$$

where $\overrightarrow{H_\mathrm{pv}}$, $\overrightarrow{H_\mathrm{so}}$ denote corresponding vectors, and the matrix Γ is

$$\mathbf{\Gamma} = \begin{pmatrix} \mathbf{A} & \mathbf{B} \\ \mathbf{B} & \mathbf{A} \end{pmatrix}. \tag{6}$$

The submatrices **A**,**B** have elements

$$A_{iajb} = (\epsilon_a - \epsilon_i)\delta_{ij}\delta_{ab} - \langle aj\ ||\ ib\rangle \tag{7}$$

$$B_{iajb} = \langle ab\ ||\ ij\rangle, \tag{8}$$

where i, j denote occupied, and a, b denote virtual orbitals.

Within a CC-LR approach [78] we have

$$E_\mathrm{pv} = \langle\langle \hat{H}_\mathrm{pv}; \hat{H}_\mathrm{so}\rangle\rangle_{\omega=0}. \tag{9}$$

The coupled-cluster wavefunction is constructed as an exponential expansion of Slater determinants:

$$|\Psi_\mathrm{CC}\rangle = e^{\hat{T}}|0\rangle, \tag{10}$$

$|0\rangle$ is the ground-state reference (Hartree–Fock) wavefunction. $\hat{T}$ denotes the standard excitation operators within the single reference coupled-cluster theory:

$$\hat{T} = \frac{1}{(n!)^2}\sum_{ijk\ldots abc\ldots} t_{ijk\ldots}^{abc\ldots} a^\dagger i b^\dagger j c^\dagger k \ldots, \tag{11}$$

which we limit to include only the singly and doubly excited determinants (CCSD). We solve the ground-state coupled-cluster equations

$$\langle 0|e^{-\hat{T}}\hat{H}e^{\hat{T}}|0\rangle = E_\mathrm{CC} \tag{12}$$

and

$$\left\langle\Phi_i^a|e^{-\hat{T}}\hat{H}e^{\hat{T}}|0\right\rangle = 0, \tag{13}$$

$$\left\langle\Phi_{ij}^{ab}|e^{-\hat{T}}\hat{H}e^{\hat{T}}|0\right\rangle = 0, \tag{14}$$

where $\hat{H}$ is the usual electronic Hamiltonian, and Φ_i^a, Φ_{ij}^{ab} denote the excited determinants. Since the coupled-cluster energy is non-variational, proper left-hand wavefunction

$$\langle \Psi_{\mathrm{CC}}| = \langle 0|(1+\hat{\Lambda})e^{-T} \tag{15}$$

is obtained from solving the so-called Λ-equations (as also required for analytic energy gradients). $\hat{\Lambda}$ is de-excitation operator similar to $\hat{T}$. The next step to form $\langle\langle \hat{H}_{\mathrm{pv}}; \hat{H}_{\mathrm{so}}\rangle\rangle_{\omega=0}$ is the solution for the perturbed wavefunction and perturbed $\hat{T}$ and $\hat{\Lambda}$ cluster operators due to SO coupling which we denote as $\hat{X}^{\omega}_{\mathrm{so}}$ and $\hat{Y}^{\omega}_{\mathrm{so}}$. These are obtained by solving the system of equations with ω being the eigenvalues of the coupled-cluster Jacobian matrix (response matrix)

$$\sum_j \langle \Phi_i|\bar{H}_N - \omega|\Phi_j\rangle \langle \Phi_j|\hat{X}^{\omega}_{\mathrm{so}}|0\rangle = -\langle \Phi_i|\bar{H}_{\mathrm{so}}|0\rangle \tag{16}$$

and

$$\sum_j \langle 0|\hat{Y}^{\omega}_{\mathrm{so}}|\Phi_j\rangle \langle \Phi_j|\bar{H}_N + \omega|\Phi_i\rangle = -\langle 0|\hat{\Lambda}[\bar{H}_{\mathrm{so}}, \tau_i]|0\rangle$$
$$-\langle 0|\hat{\Lambda}[[\bar{H}_N, \hat{X}^{\omega}_{\mathrm{so}}], \tau_i]]|0\rangle. \tag{17}$$

$\bar{H}_{\mathrm{pv}}$, $\bar{H}_{\mathrm{so}}$, $\bar{H}$ are the similarity transformed one- and two-electron operators

$$\bar{H}_{\mathrm{pv}} = e^{-T}\hat{H}_{\mathrm{pv}}e^{T}, \tag{18}$$

$$\bar{H}_{\mathrm{so}} = e^{-T}\hat{H}_{\mathrm{so}}e^{T}, \tag{19}$$

$$\bar{H} = e^{-T}\hat{H}e^{T}. \tag{20}$$

Then finally, we can form the linear-response function and compute the contributions to parity-violating potential E_{pv}

$$E_{\mathrm{pv}} = \langle\langle \hat{H}_{\mathrm{pv}}; \hat{H}_{\mathrm{so}}\rangle\rangle_{\omega=0} = \frac{1}{2}C(\pm\omega)\{\langle 0|\hat{\Lambda}[\bar{H}_{\mathrm{pv}}, \hat{X}^{\omega}_{\mathrm{so}}]|0\rangle$$
$$+\langle 0|[\hat{Y}^{\omega}_{\mathrm{so}}, \bar{H}_{\mathrm{pv}}]|0\rangle\}. \tag{21}$$

For a closed-shell reference determinant, the states determined by the coupled-cluster response theory are pure spin states, and consequently, the singlet and triplet states are also pure spin states not affected by spin contamination.

The one electron parity-violation [41] and SO integrals were implemented within PSI3 suite of quantum chemical programs [81]. Coupled-cluster response code for parity violation with a number of modules within PSI3 –‘ccenergy’, ‘cclambda’, ‘ccsort’, ‘cchbar’ – and a direct product decomposition library provide

- one- and two-electron matrix elements F_{pq}, W_{pqrs} of the coupled-cluster effective Hamiltonian;
- intermediates used in unperturbed/perturbed CCSD equations;
- intermediates used in unperturbed/perturbed Λ-equations;
- proper parametrisation of bra- and ket-vectors, and correct factorisation of intermediates contributing in the Λ-equations.

An extension of this work towards the PSI4 code [103] is in progress. We have used an uncontracted cc-pVXZ + *n*p basis sets (X = D, T, Q) augmented by sets of steep s- and p-functions. We correlate all electrons in our computations. The parity-violating potentials E_{pv} given by Equation (21) should be understood as a potential hypersurface (thus, $E_{\mathrm{pv}}(q_1, q_2, q_3, \ldots, q_{3N-6})$ depending upon all 3*N*-6 internal coordinates of the molecules [1,42]). We shall discuss here explicitly only the variation of a few coordinates, such as torsional angles. The signed electronic parity-violating energy difference $\Delta_{\mathrm{pv}}E_{\mathrm{el}}$ between the two enantiomers is defined as the difference

$$\Delta_{\mathrm{pv}}E_{\mathrm{el}}(q) = E_{\mathrm{pv}}(q, \mathrm{P})_{\mathrm{el}} - E_{\mathrm{pv}}(\overline{q}, \mathrm{M})_{\mathrm{el}}. \tag{22}$$

All values for parity-violating potentials for torsional angles $\tau = 0°–180°$ correspond to the P-enantiomer for the examples discussed below, q in Equation (22) stands for the collective set $(q_1, q_2, \ldots, q_{3N-6})$ and $\overline{q}$ to the corresponding space inverted, enantiomeric set. Because of the isotope dependence of the weak nuclear charge Q_{w}, we also note here the isotopes used consistently in all calculations reported below: H = ^{1}H, C = ^{12}C, O = ^{16}O, F = ^{19}F, S = ^{32}S, Cl = ^{35}Cl.

3. Results and discussion

As basic test case molecules for our new approach we shall first study HOOH, HSSH and ClOOCl, which have been studied before [37–43,104–107]. Figure 2 illustrates the basic structures and definition of coordinates.

The optimised geometries of HOOH, HSSH, ClOOCl are listed in Table 1. The coupled-cluster method with perturbative estimation of triples excitations CCSD(T) with correlation-consistent cc-pVXZ basis sets (X = T, D, 5) was used. Bond lengths r_e and angles α_e were kept frozen during the computation of torsional parity-violating potentials $E_{\mathrm{pv}}(\tau)$. In Figure 3, we compare the parity-violating potentials $E_{\mathrm{pv}}(\tau)$ as a function of torsional angle τ for HOOH computed with the Hartree–Fock (HF), and the coupled-cluster wavefunctions using the basis set of cc-pVQZ quality. As known from previous work, the parity-violating $E_{\mathrm{pv}}(\tau)$ has a shape of sinus-like functions which, apart from achiral *cis*- and *trans*-geometries, exhibits usually an overall non-zero contribution to E_{pv} for chiral geometries, although E_{pv} can vanish for certain chiral geometries [38–42].

The shape of these functions has been discussed before extensively [38–42], where also a qualitative explanation of the shape and the origin of zero values at chiral geometries

Table 1. The optimised molecular structures (bond lengths in pm, angles in degrees) of the ground states $\tilde{X}\ {}^1A$ structures of HOOH, HSSH and ClOOCl. Y stands for the two central atoms and X for the end position atoms (in X-Y-Y-X molecules). α is the X-Y-Y angle, τ is the dihedral angle as shown in Figure 2.

Molecule	Level	Basis set	r_e(XY)	r_e(YY)	α_e	τ_e
HOOH						
	CCSD(T)	cc-pVQZ	96.38	145.32	100.05	112.31
	CCSD(T)	cc-pV5Z	96.33	145.13	100.09	112.60
HSSH						
	CCSD(T)	cc-pVQZ	134.30	206.68	98.00	90.68
	CCSD(T)	cc-pV5Z	134.32	206.65	98.00	90.72
ClOOCl						
	CCSD(T)	cc-pVQZ	172.35	141.09	109.4	83.0
	CCSD(T)	cc-pV5Z	171.47	140.54	109.4	82.6

was given. One could mention in this context somewhat similar shapes observed in calculations of optical activity of such disulfides and dioxides (see [108] and later work also in [109,110]). Nevertheless, the analogy is not too close, as the underlying physics and the resulting operators are really quite different.

The electron correlation contributions are positive for all angles. Thus, for $\tau = 45°$ there is about 20% decrease (qualitatively, the difference is $\sim$12.00 $\times$ 10^{-20} E_h) between $E_{\rm pv}$ at the CCSD level of theory and the CPHF results. Similarly, we observe almost 20% increase for $\tau = 140°$. Thus, while the absolute values of $E_{\rm pv}$ at the minima ($\tau = 45°$) and the maxima $\tau = 135°$ are almost identical (-64.0×10^{-20} E_h vs. 60.8×10^{-20} E_h) with Hartree–Fock wavefunctions, the difference between them increases with CCSD wavefunctions. Namely, $E_{\rm pv} = -51.69 \times 10^{-20}$ E_h for $\tau = 45°$, and 76.35×10^{-20} E_h for $\tau = 135°$. Interestingly, the inclusion of electron correlation shifts the point for which the $E_{\rm pv}(\tau)$ of a chiral structure is zero. While $E_{\rm pv} = 0$ with the Hartree–Fock wavefunction at $\tau \sim 87°$, $E_{\rm pv} = 0$ at $\tau \sim 82°$ with the coupled-cluster wavefunction,

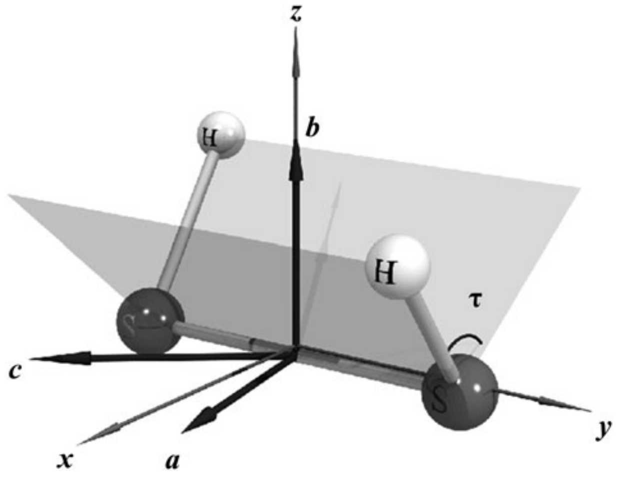

Figure 2. Equilibrium structure of H_2S_2 (P-enantiomer) as obtained with the CCSD(T) method and cc-pV5Z basis set shown in the so-called electrostatic reference frame with axes (grey) labelled x, y and z together with the so-called molecular main chiral axes [40] a, b and c (black). The equilibrium structural parameters are r_e(SS) = 207.64 pm, r_e(SH) = 134.32 pm, α_e(SSH) = 98.0°, τ_e = 90.72° (modified after [42]).

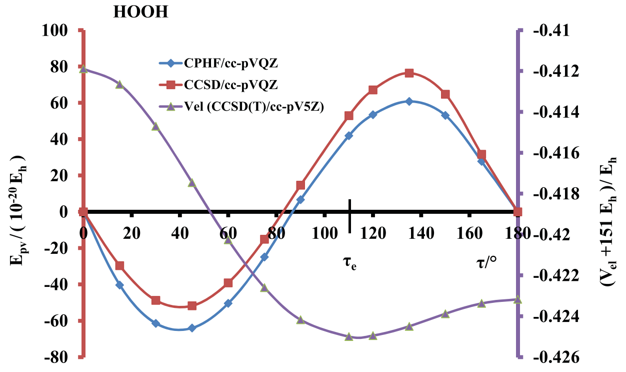

Figure 3. Parity-violating potentials $E_{\rm pv}$ as a function of τ of HOOH computed with the CPHF and CCSD-LR methods and cc-pVQZ basis set, together with the parity-conserving potential $V_{\rm el}$ computed at the CCSD(T)/cc-pV5Z level of theory.

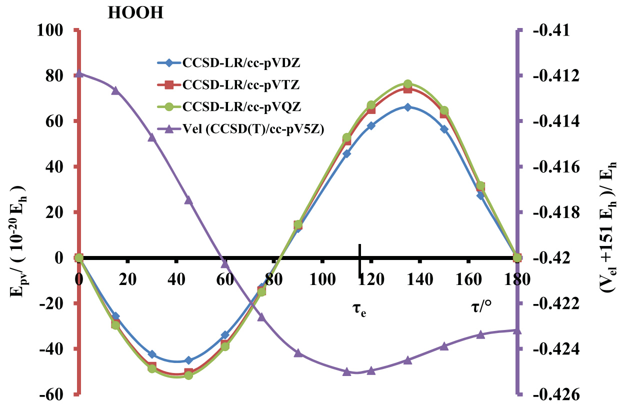

Figure 4. Parity-violating potentials $E_{\rm pv}$ as a function of τ of HOOH computed with the CCSD-LR method and various basis sets, together with the parity-conserving potential $V_{\rm el}$ computed at the CCSD(T)/cc-pV5Z level of theory.

or, expressed differently, with the Hartree–Fock wavefunction, a P-enantiomer is predicted to be more stable than the M-enantiomer for HOOH geometries up to $\tau \sim 87^\circ$; while, due to the correlation corrections, a P-enantiomer is predicted to be more stable only for geometries up to $\tau = 82^\circ$. This is of no practical relevance for the experimental detection of parity violation in HOOH, but rather (HOOH being a theoretically most investigated system for molecular parity violation) a useful example that in other molecular systems electron correlation corrections may determine which of the enantiomers should be the more stable one. The convergence of parity-violating potentials with the increase of basis sets - from double-zeta to quadruple-zeta quality, and inclusion of electron correlation at the CCSD level is demonstrated in Figure 4. The increase of basis set from double-zeta to triple-zeta-quality changes the E_{pv} values by about 10% for the extrema, but further increase to quadruple-zeta basis set changes the E_{pv} values by 5% at most, and usually not more than 3%. Overall, we can see approximate convergence being established with respect to the basis set size and the correlation treatment. Also, extensions to even larger basis sets and particularly further inclusion of electron correlation via the triple excitations (CC3 and CCSDT wavefunctions for the linear response treatment) are still feasible, but we would not expect corrections larger than a few percent. The results of various computational approaches for a prototypical system like HOOH are compared in Table 2 for $\tau = 45^\circ$ and $\Delta_{\text{pv}}E$ for the equilibrium geometry. The non-relativistic methods are listed together with the 2- and 4-component relativistic methods. There is agreement at all levels about the positive correction to the non-relativistic HF, the 2-component zeroth-order regular approximation (ZORA)–HF, and the 4-component Dirac–Coulomb HF values by higher level methods. The extent of electron correlation corrections are also comparable. This also highlights the fact that for the light molecular systems there is no reason to consider the relativistic approaches superior to the non-relativistic ones. We note rather good agreement for E_{pv} values computed with the DC-MP2 method as an analytical first-order molecular property and our E_{pv} value computed with the CCSD-LR method of -57.88×10^{-20} E$_h$ vs. -51.69×10^{-20} E$_h$. These should be probably considered superior to any values calculated as a property via methods of finite differences.

Table 2. Comparison of E_{pv} (in 10^{-20} E_h, geometry at $\tau = 45^\circ$) and $\Delta_{\text{pv}}E$ (in $10^{-14}hc$ cm^{-1}, at $\tau = 90^\circ$) for HOOH molecule computed with various methods.

Method[a]	E_{pv}	$\Delta_{\text{pv}}E^{e,l}$
SDE-RHF[b]	−1.2	0.03
CIS-RHF[c]	−39.7	3.9
CIS-LR[d]	−39.7	3.2
TDA[d]	−55.9	7.0
CPHF[e]	−61.38	2.9
RPA[f,g]	−60.88	2.8
CASSCF[g]	−45.00	3.4
DFT-B3LYP[h]	−53.56	6.5
CCSD[e]	−51.69	6.4
ZORA-HF[i]	−79.30	3.9
ZORA-B3LYP[j]	−65.40	8.3
ZORA-BLYP[j]	−69.30	9.9
DC-HF[k]	−70.60	4.0
DC-MP2[l]	−57.88	7.3
DC-CCSD(T)[m]	−61.20	8.8

[a] Note the equivalence, in principle, of the methods as given in the parentheses (CIS-RHF, CIS-LR, TDA) and (CPHF, RPA), differences arising only because of slight differences in numerical methods applied in the independent calculations by different authors.
[b] Ref. [37] [f] Ref. [111] [j] Ref. [112]
[c] Ref. [38–40,42] [g] Ref. [41] [k] Ref. [104]
[d] Ref. [43] [h] Ref. [105] [l] Ref. [106]
[e] this work [i] Ref. [113] [m] Ref. [114]

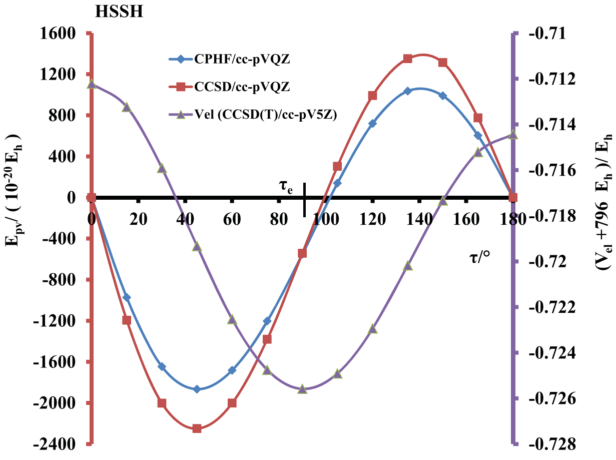

Figure 5. Parity-violating potentials E_{pv} as function of τ of HSSH computed with the CPHF and CCSD-LR methods and cc-pVQZ basis set, together with the parity-conserving potential V$_{\text{el}}$ computed at the CCSD(T)/cc-pV5Z level of theory.

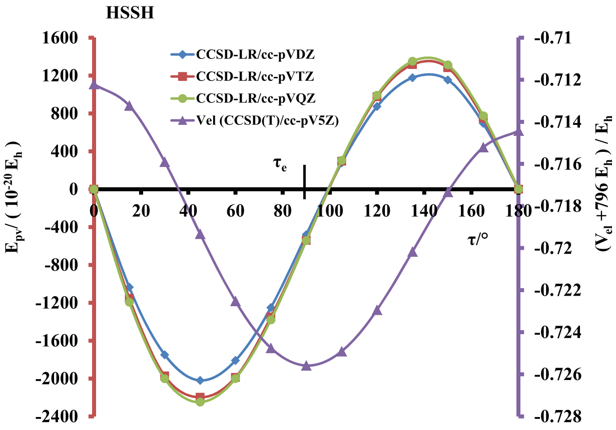

Figure 6. Parity-violating potentials E_{pv} as function of τ of HSSH computed with the CCSD-LR method and various basis sets, together with the parity-conserving potential V$_{\text{el}}$ computed at the CCSD(T)/cc-pV5Z level of theory.

Table 3. Comparison of E_{pv} (in 10^{-20} E_h, geometry at $\tau = 45°$) and $\Delta_{\text{pv}}E$ (in $10^{-14}hc$ cm^{-1}, at $\tau = 90°$) for HSSH molecule computed with various methods.

Method	E_{pv}	$\Delta_{\text{pv}}E^{\text{el}}$
SDE-RHF[a]	−135.0	2.0
CIS-RHF[b]	−1654.0	188.1
TDA[c]	−1487.7	161.5
CPHF[d]	−1865.6	242.0
RPA[e]	−1913.0	185.0
CCSD[d]	−2248.6	238.3
ZORA-HF[f]	−2350.0	294.5
ZORA-B3LYP[g]	−2690.0	290.0
ZORA-BLYP[g]	−2750.0	278.3
DC-HF[h]	−2077.0	280.0
DC-MP2[i]	−2112.0	224.3
DC-CCSD(T)[j]	−2110.0	215.1

[a] Ref. [37]
[b] Ref. [38–40,42]
[c] Ref. [43]
[d] This work
[e] Ref. [111]
[f] Ref. [113]
[g] Ref. [112]
[h] Ref. [104]
[i] Ref. [106]
[j] Ref. [114]

The parity-violating E_{pv} torsional potentials for hydrogen disulphide HSSH computed with the Hartree–Fock, and the coupled-cluster wavefunction, and cc-pVQZ quality basis set are compared in Figure 5. Different from HOOH, the correlation contributions are negative up to around $\tau = 80°$ and positive for larger angles. For the equilibrium geometry of HSSH near $\tau = 90°$, the correlation correction to E_{pv} is computed to be only $+8.5 \times 10^{-20}$ E_h (CCSD) to the value -551.5×10^{-20} E_h at the CPHF level. At the extreme points of the parity-violating potential near $\tau = 45°$ (HF value of -1866×10^{-20} E_h) and $\tau = 135°$ (CPHF value of 1036×10^{-20} E_h), the correlation corrections are -380×10^{-20} E_h (20 %) at $\tau = 45°$, and $+315 \times 10^{-20}$ E_h (30 %) at $\tau = 135°$. The extent of these corrections appears to agree more with the relativistic 2-component ZORA-based methods (see also Table 3). The convergence of parity-violating potentials as a function of τ with the increase of basis sets is demonstrated in Figure 6. As in the case of HOOH, the results obtained with the triple-zeta quality basis sets are within 5% from the quadruple-zeta quality basis set results (for large values of E_{pv}). A chiral geometry with zero contribution to E_{pv} is at a region around $\tau = 100°$ for all basis sets, and thus, the P-enantiomer of HSSH is predicted to be more stable than M-enantiomer. Various computational approaches for HSSH are compared and summarised in Table 3. Our value for $\Delta_{\text{pv}}E = (hc)\ 238.3 \times 10^{-14}$cm^{-1} at $\tau = 90°$, compares well with DC-MP2 value of $\Delta_{\text{pv}}E = (hc)\ 224.3 \times 10^{-14}$cm^{-1}. Leaving the extensively studied HXXH family of molecules, we report the parity-violating E_{pv} for ^{35}ClOO^{35}Cl and 1,3-fluoro,chloro-substituted allenes. Given the extremely small tunnelling splittings in the ground state, ClOOCl and 1,3 difluoroallene were identified earlier [107,115] as potential candidates for the experimental detection of the parity-violating energy difference between the enantiomers. Parity-violating potentials $E_{\text{pv}}(\tau)$ for ClOOCl [107] have been previously computed with the random phase approximation (RPA) method (qualitatively equal to the CPHF method), and multiconfigurational self consistent field (MCSCF-LR) approach was used to characterise 1,3 difluoroallene [115]. The parity-violating potentials $E_{\text{pv}}(\tau)$ of ClOOCl computed with the Hartree–Fock, and coupled-cluster wavefunctions and cc-pVQZ basis set are compared in Figure 7. Different from the the previous cases, there is no chiral geometry of ClOOCl at which one finds $E_{pv} = 0$. The M-enantiomer is thus predicted to be more stable than the P-enantiomer for all torsional angles. Curiously, the correlation correction is positive for all angles apart from the region with τ from 100° to 120°. Furthermore, it never exceeds more than 10% apart from the region τ from 40° to 80°, where the correlation correction increases towards 20%. The convergence of parity-violating potentials with the increase of basis sets is documented by Figure 8. Though the increase of basis set from double-zeta

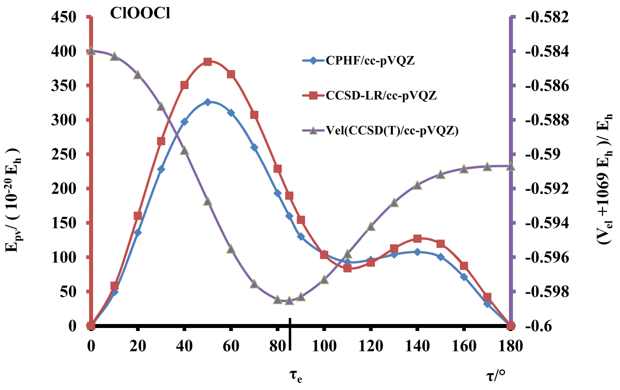

Figure 7. Parity-violating potentials E_{pv} as function of τ of ClOOCl computed with the CPHF and CCSD-LR methods, and cc-pVQZ basis set, together with the parity-conserving potential V_{el} computed at the CCSD(T)/cc-pVQZ level of theory.

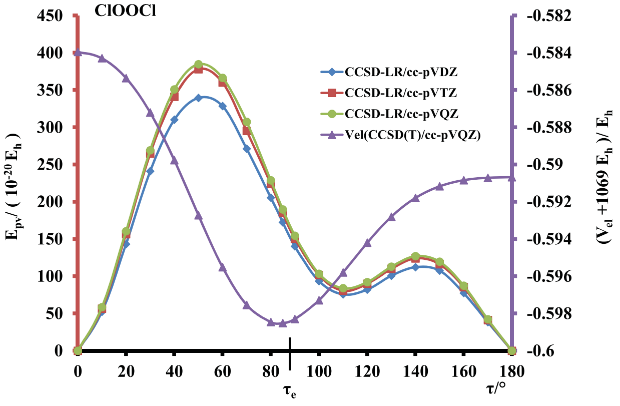

Figure 8. Parity-violating potentials E_{pv} as function of τ of ClOOCl computed with the CCSD-LR method and various basis sets, together with the parity-conserving potential V_{el} computed at the CCSD(T)/cc-pVQZ level of theory.

Table 4. The optimised molecular structures (bond lengths in pm, angles in degrees) of the ground state of 1,3 difluoroallene and 1,3 dichloroallene.

Molecule	Parameter	MP2/ cc-pVQZ	CCSD(T)/ cc-pVTZ
1,3 difluoroallene			
	r_e(CC)	130.25	130.98
	r_e(CF)	134.12	134.30
	r_e(CH)	107.94	108.16
	∠(CCC)	176.88	177.26
	∠(FCC)	122.52	122.50
	∠(HCC)	124.98	124.75
1,3 dichloroallene			
	r_e(CC)	130.35	130.95
	r_e(CCl)	172.78	174.32
	r_e(CH)	107.93	108.06
	∠(CCC)	180.00	180.00
	∠(ClCC)	122.54	122.67
	∠(HCC)	123.26	123.26

Table 5. The optimised molecular structures (bond lengths in pm, angles in degrees) of the ground state of 1,fluoro,3 chloroallene.

Parameter	MP2/cc-pVQZ	CCSD(T)/cc-pVTZ
r_e(CC)	130.33	130.99
r_e(CF)	134.11	134.29
r_e(CCl)	172.95	174.49
r_e(CH)	107.94	108.11
∠(CCC)	177.05	177.36
∠(FCC)	122.69	122.63
∠(ClCC)	122.59	122.72
∠(HCC)	124.05	123.96

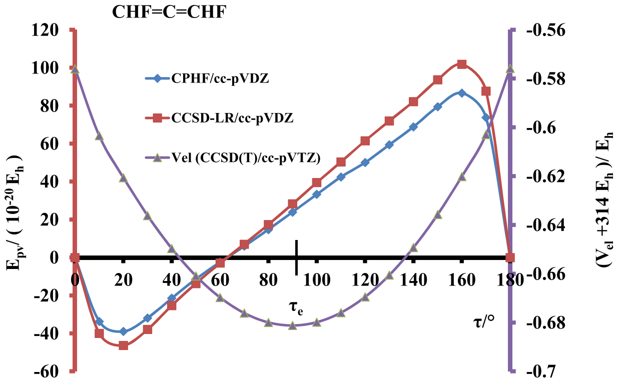

Figure 9. Parity-violating potentials E_{pv} as function of τ for 1,3 difluoroallene computed with the CPHF and CCSD-LR methods, and cc-pVDZ basis set, together with the parity-conserving potential V_{el} computed at the CCSD(T)/cc-pVTZ level of theory.

to triple-zeta quality at given level of theory results in about 10% change, further increase of basis set to quadruple-zeta quality leads to changes of only 2% beyond this. CCSD/cc-pVQZ level of theory calculations with the unfrozen core of ClOOCl are also together with 1,3 dichloroallene among the most extensive computations we report here. At this level, we predict the M-enantiomer to be stabilised compared with the P-enantiomer by $\Delta_{\mathrm{pv}}E = (hc)\ 91 \times 10^{-14}\mathrm{cm}^{-1}$, which can be compared with previously reported $\Delta_{\mathrm{pv}}E = (hc)\ 60 \times 10^{-14}\mathrm{cm}^{-1}$ obtained with the RPA method.

Table 4 and 5 list the optimised geometries of 1,3 difluoroallene, 1,3 dichloroallene and 1,fluoro,3 chloroallene. The parity-violating potentials $E_{\mathrm{pv}}(\tau)$ computed for 1,3 difluoroallene at the CPHF and CCSD-LR levels of theory with double-zeta quality basis set are shown in Figure 9. Apart from two pronounced maxima at $\tau = 20°$ and $\tau = 160°$, the correlation contributions do not exceed 10%, they are negative for the geometries up to $\tau = 60°$, and positive for larger angles. The parity-violating potentials $E_{\mathrm{pv}}(\tau)$ for 1,fluoro,3 chloro-allene are shown in Figure 10, and for 1,3 dichloroallene in Figure 11. The correlation corrections are relatively small for these examples, similar among all allenes we studied. The comparison of results for the substituted allenes and series of basis sets are presented in Figures 12–14. Very little dependence of parity-violating torsional potentials with respect to basis set size is observed. Thus, the fluoro,chloro-substituted allenes can be seen as special examples of molecules where the parity violation is strongly determined by geometry (τ), and very little dependent on the level of theory used when computed as a response property. Finally, the parity-violating potentials $E_{\mathrm{pv}}(\tau)$ for all three allenes are compared in Figure 15. The M-enantiomer is computed to be stabilised with respect to the P-enantiomer by $\Delta_{\mathrm{pv}}E = (hc)\ 14 \times 10^{-14}\mathrm{cm}^{-1}$ for 1,3 difluoroallene, which can be compared with previously reported $\Delta_{\mathrm{pv}}E = (hc)\ 12.9 \times 10^{-14}\mathrm{cm}^{-1}$ [115]. The M-enantiomer of 1,fluoro,3 chloroallene is predicted to be more stable than the P-enantiomer by $\Delta_{\mathrm{pv}}E = (hc)\ 7.1 \times 10^{-13}\mathrm{cm}^{-1}$, and the M-enantiomer of 1,3 dichloroallene is predicted to be more stable than the P-enantiomer by

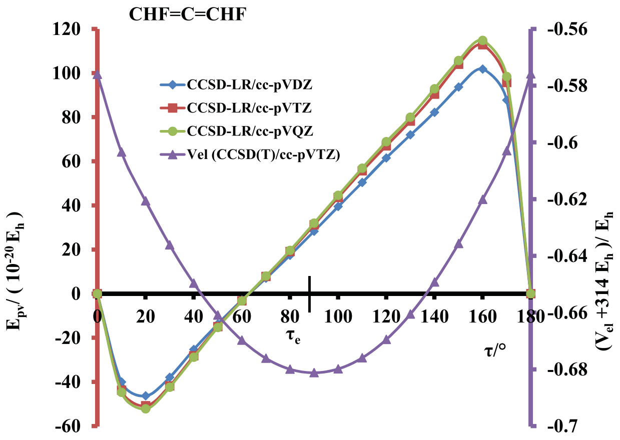

Figure 10. Parity-violating potentials E_{pv} as function of τ of 1,3 difluoroallene computed with the CCSD-LR method and various basis sets, together with the parity-conserving potential V_{el} computed at the CCSD(T)/cc-pVTZ level of theory.

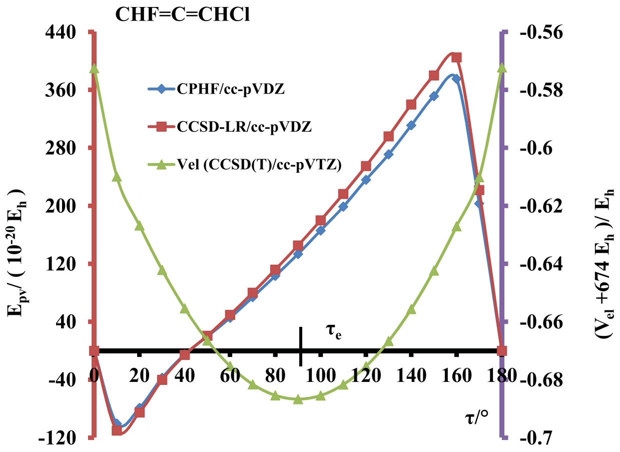

Figure 11. Parity-violating potentials E_{pv} as function of τ for 1,fluoro,3 chloroallene computed with the CPHF, and CCSD-LR methods and cc-pVDZ basis set, together with the parity-conserving potential V_{el} computed at the CCSD(T)/cc-pVTZ level of theory.

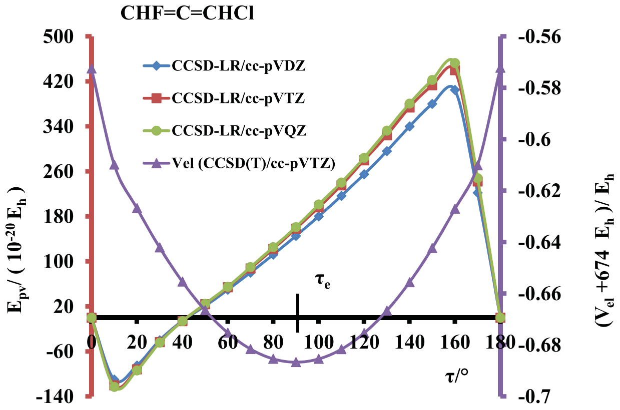

Figure 12. Parity-violating potentials E_{pv} as function of τ for 1,fluoro,3 chloroallene computed with the CPHF and CCSD-LR methods, and cc-pVDZ basis set, together with the parity-conserving potential V_{el} computed at the CCSD(T)/cc-pVTZ level of theory.

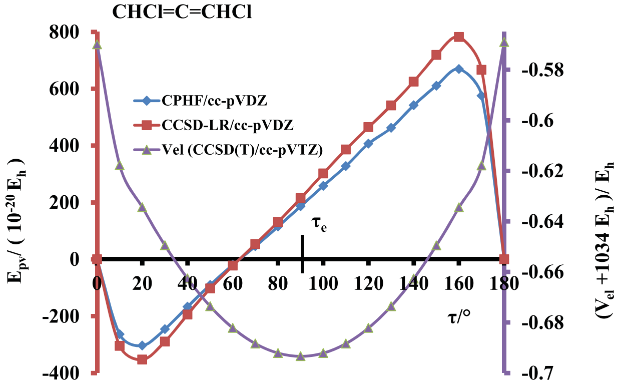

Figure 13. Parity-violating potentials E_{pv} as function of τ for 1,3 dichloroallene computed with the CPHF and CCSD-LR methods, and cc-pVDZ basis set, together with the parity-conserving potential V_{el} computed at the CCSD(T)/cc-pVTZ level of theory.

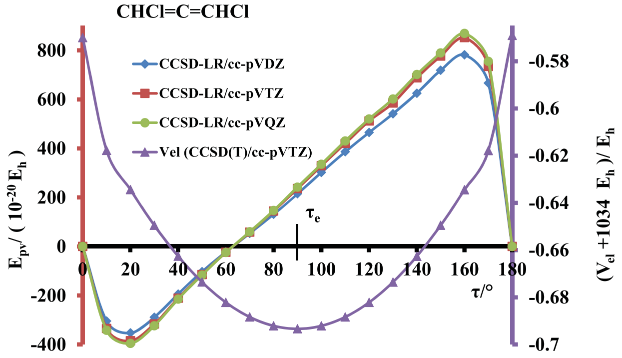

Figure 14. Parity-violating potentials E_{pv} as function of τ of 1,3 dichloroallene computed with the CCSD-LR method and various basis sets, together with the parity-conserving potential V_{el} computed at the CCSD(T)/cc-pVTZ level of theory.

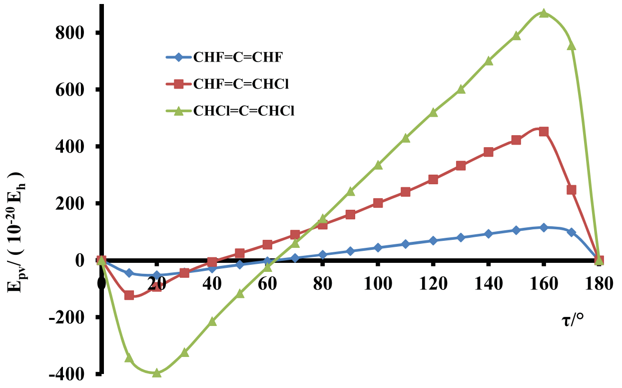

Figure 15. Comparison of parity-violating potentials E_{pv} as function of τ of 1,3 difluoroallene, 1,fluoro,3 chloroallene, and 1,3 dichloroallene computed with the CCSD-LR method and cc-pVQZ basis set.

$\Delta_{\mathrm{pv}}E = (hc)\ 1.1 \times 10^{-12}\mathrm{cm}^{-1}$ at the respective equilibrium geometries. The latter allene is thus a quite suitable candidate for an approach to measure $\Delta_{\mathrm{pv}}E$ using the excited electronic state as intermediate in the approach of [24,25], provided that the high-resolution electronic spectra show sufficiently resolved rovibronic lines structure. Obviously, the relatively heavy chlorine substituent with nuclear quadrupole moments and resulting complex hyperfine structures will lead to complex spectra, which are, however, in principle, resolvable [49].

4. Conclusions

The effects arising from parity violation in chiral molecules and, in particular, the parity-violating energy difference $\Delta_{\mathrm{pv}}E$ between the enantiomers can be considered among the most fundamental new aspects and in part unsolved questions in stereochemistry and even biomolecular evolution, even in a broad historical perspective [116,117]. We can summarise the approach towards solving this problem in the following steps.

(1) Obtain approximate results for $\Delta_{\mathrm{pv}}E$ from realistic theoretical calculations on selected molecules, which may serve as candidates for spectroscopic experiments towards molecular parity violation (testing also theoretically for possible effects due to tunnelling).
(2) Carry out the necessary spectroscopic experiments and rovibrational analyses [118,119] on these molecules in order to identify and assign (with respect to rovibrational symmetry and parity) appropriate spectral lines for the relevant experiment (as schematically summarised in Figure 1).
(3) Carry out the experiments along one or several of the lines outlined schematically in Figure 1 to obtain an experimental value of $\Delta_{\mathrm{pv}}E$. This will provide a test of the validity of the theory.
(4) Analyse the experimental results for $\Delta_{\mathrm{pv}}E$ by means of highly accurate theoretical calculation to extract fundamental parameters of the standard model (SMPP), for instance in view of a possible energy dependence of the Weinberg angle [1] (this also needs the inclusion of rovibrational effects on $\Delta_{\mathrm{pv}}E$ [18]).
(5) Use accurate calculations by means of the theoretically well established and experimentally checked methods to predict relevant quantities arising from parity violation in possible mechanisms of biomolecular evolution in order to establish (or refute) the influence of molecular parity violation [1,16,117].

This work contributes to the first and last two steps of such a project. The coupled-cluster techniques developed here allow for further refinement towards much higher accuracy. At present, the specific results presented here provide sufficiently reliable estimates on the molecules studied to decide upon their possible use in experiments. While, in principle, calculations of tunnelling splittings $\Delta E_{\pm}$ in the ground state would be necessary in addition, these can be omitted for the molecules studied here, as they fall clearly into the two limiting cases $\Delta_{\mathrm{pv}}E \ll \Delta E_{\pm}$ (H_2O_2, H_2S_2, unsuitable for experiments on $\Delta_{\mathrm{pv}}E$) and $\Delta_{\mathrm{pv}}E \gg \Delta E_{\pm}$ (ClOOCl [107] and substituted allenes, in principle, all suitable for experiments on $\Delta_{\mathrm{pv}}E$). From the numerical results, in particular, 1,3 dichloroallene is a good candidate for such experiments if the spectroscopic difficulties can be resolved. As already pointed out [115], $\Delta_{\mathrm{pv}}E$ of 1,3 difluoroallene is exceptionally small, making this a difficult case, and 1,fluoro,3 chloroallene is intermediate and thus a borderline candidate molecule.

From this work, it is also seen that correlation contributions can be substantial and have to be taken into account in realistic calculations of $\Delta_{\mathrm{pv}}E$. The implementation of efficient coupled-cluster methods in this work will prove useful for many future applications and further work on suitable candidate molecules is in progress as is also the work on further improvement of the theory towards highly accurate results in view of step 4 of the overall approach.

Acknowledgements

Our work has profited from help and discussions with past and current members of our group, in particular, Sieghard Albert, Robert Berger, Csaba Fábri, Eduard Miloglyadov, Georg Seyfang, Jürgen Stohner and Martin Willeke. This work was supported by ETH Zürich; the Swiss National Science Foundation; an ERC Advanced Grant [grant number 290925]. In particular, the research leading to these results has received funding from the European Research Council under the European Union's Seventh Framework Programme [FP7 2007- 5302013].

Disclosure statement

No potential conflict of interest was reported by the authors.

References

[1] M. Quack, Fundamental Symmetries and Symmetry Violations in High-resolution Spectroscopy. in *Handbook of High Resolution Spectroscopy*, edited by F. Merkt and M. Quack (John Wiley & Sons, Ltd., Chichester, New York, 2011), pp. 659–722.
[2] M.A. Bouchiat and C. Bouchiat, J. Phys. **35** (12), 899–927 (1974).
[3] M.A. Bouchiat and C. Bouchiat, J. Phys. **36** (6), 493–509 (1975).
[4] S. Weinberg, Phys. Rev. Lett. **19** (21), 1264–1266 (1967).
[5] S.L. Glashow, Nucl. Phys. **22** (4), 579–588 (1961).
[6] A. Salam, Elementary Particle Theory, in *Proc. 8th Nobel Symposium* (Almqvist and Wiksell, Stockholm, 1968), pp. 367–377.
[7] M.J.G. Veltman, Rev. Mod. Phys. **72**, 341 (2000).
[8] G. 't Hooft, Rev. Mod. Phys. **72**, 333 (2000).
[9] S.C. Bennett and C.E. Wieman, Phys. Rev. Lett. **82** (12), 2484–2487 (1999).
[10] T.D. Lee and C.N. Yang, Phys. Rev. **104** (1), 254–258 (1956).
[11] C.S. Wu, E. Ambler, R.W. Hayward, D.D. Hoppes, and R.P. Hudson, Phys. Rev. **105** (4), 1413–1415 (1957).
[12] R.L. Garwin, L.M. Lederman, and M. Weinrich, Phys. Rev. **105** (4), 1415–1417 (1957).
[13] J.I. Friedman and V.L. Telegdi, Phys. Rev. **105**, 1681 (1957).
[14] Y. Yamagata, J. Theor. Biol. **11**, 495 (1966).
[15] D.W. Rein, J. Mol. Evolution **4**, 15 (1974).
[16] M. Quack, Angew. Chem. Int. Ed. **41** (24), 4618–4630 (2002).
[17] M. Quack and J. Stohner, Phys. Rev. Lett. **84** (17), 3807–3810 (2000).
[18] M. Quack and J. Stohner, J. Chem. Phys. **119** (21), 11228–11240 (2003).
[19] V. Letokhov, Phys. Lett. A **53** (4), 275–276 (1975).
[20] O. Kompanets, A. Kukudzhanov, V. Letokhov, and L. Gervits, Opt. Commun. **19**, 414 (1976).
[21] E. Arimondo, P. Glorieux, and T. Oka, Opt. Commun. **23**, 369 (1977).
[22] R. Harris and L. Stodolsky, Phys. Lett. B **78**, 313 (1978).
[23] R. Harris and L. Stodolsky, J. Chem. Phys. **74**, 2145 (1981).
[24] M. Quack, Chem. Phys. Lett. **132** (2), 147–153 (1986).

[25] M. Quack, Angew. Chem. Int. Ed. **28** (5), 571–586 (1989).

[26] M.J.M. Pepper, I. Shavitt, P. v. Ragué Schleyer, M.N. Glukhovtsev, R. Janoschek, and M. Quack, J. Comp. Chem. **16**, 207 (1995).

[27] A. Bauder, A. Beil, D. Luckhaus, Müller, and M. Quack, J. Chem. Phys. **106**, 7558 (1997).

[28] M. Quack and J. Stohner, Chirality **13** (10), 745–753 (2001).

[29] C. Daussy, T. Marrel, A. Amy-Klein, C.T. Nguyen, C. Bordé, and C. Chardonnet, Phys. Rev. Lett. **83** (8), 1554–1557 (1999).

[30] M. Ziskind, C. Daussy, T. Marrel, and C. Chardonnet, Eur. Phys. J. D **20**, 219 (2002).

[31] J. Crassous, F. Monier, J.P. Dutasta, M. Ziskind, C. Daussy, C. Grain, and C. Chardonnet, ChemPhysChem **4**, 541 (2003).

[32] M. Schnell and J. Küpper, Faraday Discuss. **150**, 33 (2011).

[33] M. Quack, Faraday Discuss. **150**, 533 (2011).

[34] S.K. Tokunaga, C. Stoeffler, F. Auguste, A. Shelkovnikov, C. Daussy, A. Amy-Klein, C. Chardonnet, and B. Darquié, Mol. Phys. **111**, 2363 (2013).

[35] R.A. Hegstrom, D.W. Rein, and P.G. Sandars, J. Chem. Phys. **73** (5), 2329–2341 (1980).

[36] S.F. Mason and G.E. Tranter, Chem. Phys. Lett. **94** (1), 34–37 (1983).

[37] S.F. Mason and G.E. Tranter, Mol. Phys. **53** (5), 1091–1111 (1984).

[38] A. Bakasov, T.K. Ha, and M. Quack, Ab initio calculations of molecular energies including parity violating energies. in *Proc. of the 4th Trieste Conference (1995), Chemical Evolution: Physics of the Origin and Evolution of Life*, edited by J. Chela-Flores and F. Raulin (Kluwer Academic Publishers, Dordrecht, 1996), p. 287.

[39] A. Bakasov, T. Ha, and M. Quack, J. Chem. Phys. **109** (17), 7263–7285 (1998).

[40] A. Bakasov and M. Quack, Chem. Phys. Lett. **303** (5–6), 547–557 (1999).

[41] R. Berger and M. Quack, J. Chem. Phys. **112** (7), 3148–3158 (2000).

[42] A. Bakasov, R. Berger, T. Ha, and M. Quack, Int. J. Quant. Chem. **99** (4), 393–407 (2004).

[43] P. Lazzeretti and R. Zanasi, Chem. Phys. Lett. **279**, 349 (1997).

[44] J.K. Laerdahl, P. Schwerdtfeger, and H.M. Quiney, Phys. Rev. Lett. **84** (17), 3811–3814 (2000).

[45] M. Quack and J. Stohner, Chimia **59** (7–8), 530–538 (2005).

[46] R. Berger, in *Relativistic Electronic Structure Theory, Part II- Applications*, edited by P. Schwerdtfeger (Elsevier, Netherlands, 2004), pp. 188–288.

[47] M. Quack, J. Stohner, and M. Willeke, Ann. Rev. Phys. Chem. **59**, 741 (2008).

[48] R. Bast, A. Koers, A.S.P. Gomes, M. Iliaš, L. Visscher, P. Schwerdtfeger, and T. Saue, Phys. Chem. Chem. Phys. **13**, 864 (2011).

[49] P. Dietiker, E. Miloglyadov, M. Quack, A. Schneider, and G. Seyfang, Two Photon IR-Laser Induced Population Transfer in NH (index 3) - First Steps to Measure Parity Violation in Chiral Molecules. in *Proc. of the 19th Symposium on Atomic, Cluster and Surface Physics 2014 (SASP 2014)*, edited by D. Stock, R. Wester and P. Scheier (Innsbruck University Press, Innsbruck, 2014), pp. 226–229.

[50] J. Čížek, J. Chem. Phys. **45**, 4256 (1966).

[51] F. Coester and H. Kümmel, Nucl. Phys. **17**, 477 (1960).

[52] O. Sinanoğlu, J. Chem. Phys. **36**, 706 (1962).

[53] J. Paldus, J. Čížek, and I. Shavitt, Phys. Rev. A **5**, 50 (1972).

[54] J. Paldus and J. Čížek, Adv. Quantum Chem. **9**, 106 (1975).

[55] D. Mukherjee and S. Pal, Adv. Quantum Chem. **20**, 291 (1989).

[56] T.D. Crawford and H.F. Schaefer, Rev. Comp. Chem. **14**, 33 (2000).

[57] J. Paldus, in *Theory and Applications of Computational Chemistry: The First Forty Years*, edited by C.E. Dykstra, G. Frenking and K.S. Kim (Elsevier, Amsterdam, 2005), pp. 115–147.

[58] R.J. Bartlett, in *Theory and Applications of Computational Chemistry: The First Forty Years*, edited by C.E. Dykstra, G. Frenking and K.S. Kim (Elsevier, Amsterdam, 2005), p. 1191.

[59] R.J. Bartlett, and M. Musial, Rev. Mod. Phys. **79**, 291 (2007).

[60] F.E. Harris, H.J. Monkorst, and D.L. Freeman, *Algebraic and Diagrammatic Methods in Many-Fermion Theory* (Oxford University Press, New York, 1992).

[61] I. Shavitt and R.J. Bartlett, *Many-Body Methods in Chemistry and Physics: MBPT and Coupled-Cluster Theory* (Cambridge Uninversity Press, Cambridge, 2009).

[62] J. Paldus, P. Čársky and J. Pittner, in *Recent Progress in Coupled Cluster Methods*, edited by J. Paldus, P. Čársky and J. Pittner, Conference Series (Springer, Dordrecht, 2010).

[63] M. Reiher and A. Wolf, *Relativistic Quantum Chemistry* (Wiley, VCH, Weinheim, 2009).

[64] H.J. Monkhorst, Int. J. Quantum Chem. Symp. **103**, 7429 (1977).

[65] D. Mukherjee and P.K. Mukherjee, Chem. Phys. **39**, 325 (1979).

[66] S. Ghosh, D. Mukherjee, and S.N. Bhattacharya, Chem. Phys. **72**, 161 (1982).

[67] H. Sekino and R.J. Bartlett, Int. J. Quantum Chem. Symp. **18**, 255 (1984).

[68] H. Koch and P. Jørgensen, J. Chem. Phys. **93** (5), 3333–3344 (1990).

[69] H. Koch, H.J.A. Jensen, P. Jørgensen, and T. Helgaker, J. Chem. Phys. **93** (5), 3345–3350 (1990).

[70] J.F. Stanton and R.J. Bartlett, J. Chem. Phys. **98**, 7029 (1993).

[71] J.F. Stanton and R.J. Bartlett, J. Chem. Phys. **99**, 5178 (1993).

[72] J. Paldus, P. Piecuch, L. Pylypow, and B. Jeziorski, Phys. Rev. A **47**, 2738 (1993).

[73] P. Piecuch, S. Kucharski, and R.J. Bartlett, J. Chem. Phys. **110**, 6103 (1999).

[74] K. Ruud and T. Helgaker, Chem. Phys. Lett. **352**, 533 (2002).

[75] T.D. Crawford, Theor. Chem. Acc. **115**, 227 (2006).

[76] T.D. Crawford, M.C. Tam, and M.L. Abrams, J. Phys. Chem. A **111**, 12057 (2007).

[77] O. Christiansen, H. Koch, and P. Jørgensen, Chem. Phys. Lett. **243**, 409 (1995).

[78] T. Helgaker, S. Coriani, P. Jørgensen, K. Kristensen, J. Olsen, and K. Ruud, Chem. Rev. **112**, 543 (2012).

[79] R. McWeeny, *Methods of Molecular Quantum Mechanics* (Academic Press, London, 1989).

[80] Y. Yamaguchi, Y. Osamura, J.D. Goddard and H.F. Schaefer, *A New dimension to Quantum Chemistry. Analytic Derivative Methods in Ab initio Molecular Electronic Structure Theory* (Oxford University Press, New York, 1994).

[81] T.D. Crawford, C.D. Sherrill, E.F. Valeev, J.T. Fermann, R.A. King, M.L. Leininger, S.T. Brown, C.L. Janssen, E.T. Seidl, J.P. Kenny, and W.D. Allen, J. Comput. Chem. **28** (9), 1610–1616 (2007).

[82] A. Willets, J.F. Gaw, S. Carter, and N.C. Handy, J. Mol. Spectrosc. **135**, 370 (1989).

[83] M.J. Bramley and N.C. Handy, J. Chem. Phys. **98**, 1378 (1993).

[84] B. Kuhn, T.R. Rizzo, D. Luckhaus, M. Quack, and M.A. Suhm, J. Chem. Phys. **111**, 2565 (1999).

[85] B. Fehrensen, D. Luckhaus, and M. Quack, Chem. Phys. Lett. **300**, 312 (1999).

[86] B. Fehrensen, D. Luckhaus, and M. Quack, Chem. Phys. **338**, 90 (2007).

[87] L. Horný and M. Quack, Faraday Discuss. **150**, 152 (2011).

[88] A.L. Barra, J.B. Robert, and L. Wiesenfeld, Phys. Lett. A **115** (9), 443–447 (1986).

[89] E. Fermi, Z. Phys. **88**, 161 (1934).

[90] A.L. Barra, J.B. Robert, and L. Wiesenfeld, BioSystems **20**, 57 (1987).

[91] G. Laubender and R. Berger, Chem Phys Chem **4**, 395 (2003).

[92] G. Laubender and R. Berger, Phys. Rev. A **74**, 032105 (2006).

[93] V. Weijo, M.B. Hansen, O. Christiansen, and P. Manninen, Chem. Phys. Lett. **470**, 166 (2009).

[94] F. Hobi, R. Berger, and J. Stohner, Mol. Phys. **111**, 2345 (2013).

[95] B. Zel'dovich, D. Saakyan, and I. Sobel'man, Sov. Phys. JETP **25** (2), 94 (1977).

[96] W. Pauli, Z. Phys. **43**, 601 (1927).

[97] G. Breit, Phys. Rev. **34**, 553 (1929).

[98] G. Breit, Phys. Rev. **36**, 383 (1930).

[99] G. Breit, Phys. Rev. **39**, 616 (1932).

[100] S. Koseki, M.W. Schmidt, and M.S. Gordon, J. Phys. Chem. **96**, 10768 (1992).

[101] S. Koseki, M.S. Gordon, M.W. Schmidt, and N. Matsunaga, J. Phys. Chem. **99**, 12764 (1995).

[102] R. Berger, Angew. Chem. Int. Ed. **43** (4), 398–401 (2004).

[103] J.M. Turney, A.C. Simmonett, R.M. Parrish, E.G. Hohenstein, F.A. Evangelista, J.T. Fermann, B.J. Mintz, L.A. Burns, J.J. Wilke, M.L. Abrams, N.J. Russ, M.L. Leininger, C.L. Janssen, E.T. Seidl, W.D. Allen, H.F. Schaefer, R.A. King, E.F. Valeev, C.D. Sherrill, and T.D. Crawford, WIREs Comput Mol Sci. **2** (4), 556 (2012).

[104] J.K. Laerdahl and P. Schwerdtfeger, Phys. Rev. A **60** (6), 4439–4453 (1999).

[105] A.C. Hennum, T. Helgaker, and W. Klopper, Chem. Phys. Lett. **354**, 274 (2002).

[106] J.N.P. van Stralen, L. Visscher, C.V. Larsen, and H.J.A. Jensen, Chem. Phys. **311**, 81 (2005).

[107] M. Quack and M. Willeke, J. Phys. Chem. A **110** (9), 3338–3348 (2006).

[108] J. Linderberg and J. Michl, J. Am. Chem. Soc. **92**, 2619 (1970).

[109] J. Hutter, H.P. Lüthi, and T.K. Ha, J. Mol. Struct. **234**, 515 (1991).

[110] T.K. Ha and W. Cencek, Chem. Phys. Lett. **182**, 519 (1991).

[111] R. Berger, J. Phys. Chem. **129**, 154105 (2008).

[112] R. Berger and C. van Wüllen, J. Chem. Phys. **122** (13), 134316 (2005).

[113] R. Berger, N. Langermann, and C. van Wüllen, Phys. Rev. A **71** (4), 042105 (2005).

[114] J. Thyssen, J.K. Laerdahl, and P. Schwerdtfeger, Phys. Rev. Lett. **85** (15), 3105–3108 (2000).

[115] M. Gottselig and M. Quack, J. Chem. Phys. **123** (8), 084305 (2005).

[116] M. Quack, Eur. Rev. **22**, S50 (2014).

[117] M. Quack, Adv. Chem. Phys. **157**, 97 (2014).

[118] S. Albert and M. Quack, Nachrichten aus der Chemie **62**, 313 (2014).

[119] S. Albert, K. Albert Keppler and M. Quack, High Resolution Fourier Transform Infrared Spectroscopy. in *Handbook of High Resolution Spectroscopy*, edited by F. Merkt and M. Quack (John Wiley & Sons, Ltd., Chichester, New York, 2011), pp. 965–1020.